Aust. J. Phys., 1990, **43**, 651–64

Photoelectron Spectroscopy of Solids — VUV Bandstructure Studies*

Robert Leckey and John Riley

Physics Department and Research Centre for Electron Spectroscopy,
La Trobe University, Bundoora, Vic. 3083, Australia.

Abstract

The electronic bandstructure of solids, including states specific to the surface, may now be explored in very great detail by photoelectron spectroscopy. Variable energy photon sources (synchroton radiation sources) coupled with advanced angle resolving electron spectrometers permit access to emission from specific points within the complete Brillouin zone. The technique of band mapping has now reached a stage where the small $\boldsymbol{k}$-dependent changes to individual valence bands due to the effects of introduced lattice strain can be observed, for example. The relative importance of emission from surface states, as opposed to bulk band states, can be demonstated dramatically using off-normal emission data. Angle resolved constant initial state spectroscopy has recently been shown to provide details of excited state bandstructure and has clarified the involvement of surface and bulk Umklapp scattering in the photoemission process. The above capabilities of photoelectron spectroscopy are discussed, using metallic and semiconducting examples, and are related to interface problems in general.

1. Introduction

Detailed knowledge of the electronic structure of materials is the key to an understanding of their electrical, optical and magnetic behaviour and is of equal importance in the study of both their chemical behaviour and their geometrical structure. It has long been recognised that the existence of a surface or the presence of an interface between two different materials, opens up the possibility of a new family of electronic states which would not exist in an infinite solid.

It is sufficient here to stress that it is these surface states which often play a predominant role in controlling surface reactivity (to take a chemical example) and in establishing the magnitude of the Schottky barrier height between metal and a semiconductor (to take a physical example).

The pre-eminent technique for the determination of the electronic bandstructure—both bulk and surface—of materials is angle resolved photo-

* Paper presented at the Workshop on Interfaces in Molecular, Electron and Surface Physics, held at Fremantle, Australia, 4–7 February 1990.

0004-9506/90/040651$03.00

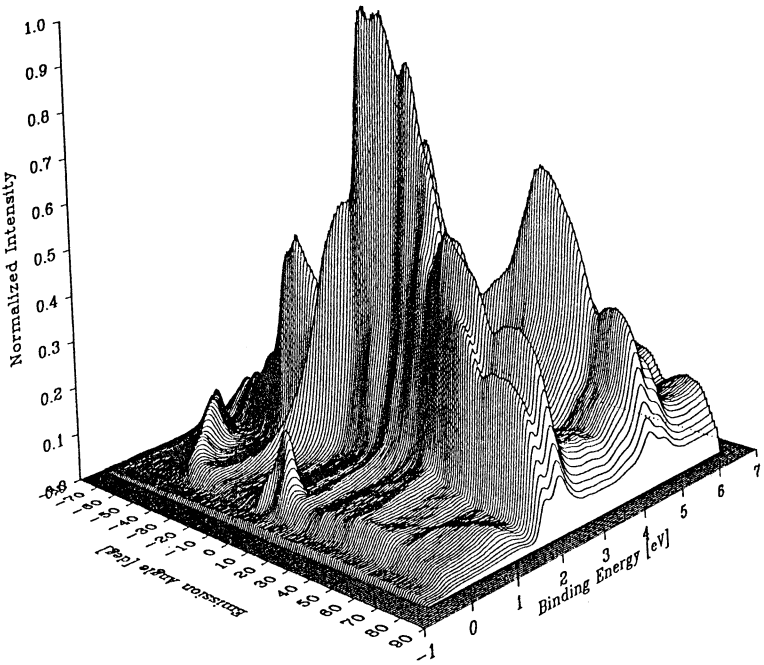

Fig. 1. Angle resolved photoemission from Cu(111) in the [11$\bar{2}$] azimuth taken with p-polarised light of 26 eV energy directed at 45° to the sample normal.

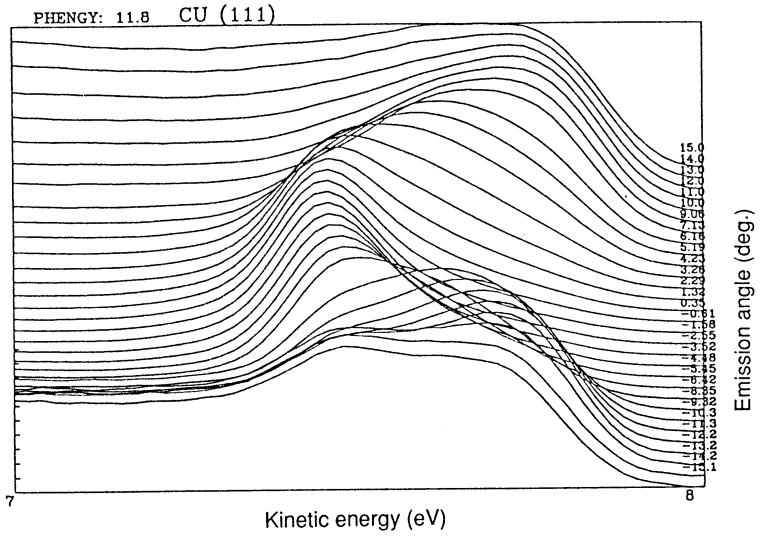

Fig. 2. Detailed dispersion of the surface state at Γ seen in Fig. 1.

electron spectroscopy (ARUPS). The aim of such experiments is to establish the form of the $E(\boldsymbol{k})$ bandstructure, for general points $\boldsymbol{k}$ within the Brillouin zone, covering a complete valence/conduction band. A typical range of binding energies for occupied states is $0 < E \leq 10$ eV. This implies that an energy resolution ΔE in the vicinity of 50–100 meV and a momentum resolution $\Delta k \approx 0 \cdot 05$ Å^{-1} are required. The latter requirement constrains the maximum photon energy which can sensibly be used for such an experiment to values below approximately 100 eV especially if the photon source is unpolarised. Band mapping experiments using photoemission are consequently best carried out on what are normally described as UV beamlines at synchrotron radiation sources. In purely laboratory terms, the use of XPS energies is not indicated for this class of experiment. The use of laboratory UV sources (He I, II; Ne I, II) can provide valuable bandstructure information as shown below, but such fixed photon energy sources have severe limitations.

2. ARUPS Experiments

The ARUPS experiments which will be described here have been performed using a toroidal electron energy analyser specifically designed for bandmapping experiments (Leckey and Riley 1985; Toffoletto *et al.* 1985). Its particular advantage is the ability to acquire data in parallel for electrons emitted at all polar angles $\theta \leq \pm 90°$ from a single crystal sample. Under normal conditions, it is operated with $\Delta E = 80$ meV and $\Delta\theta = \pm 1°$. A typical data set, $N(E, \theta)$, obtained in about 20 minutes on the TGM-4 beamline at the Berlin Synchrotron Radiation Source (BESSY) is shown in Fig. 1.

This diagram is included to indicate the various types of bands which may be identified simply by inspection. Thus, emission from the Cu (3d) bands dominates the data (for cross-sectional reasons) and is readily identified due to the fact that the real-space localisation of these electrons implies little dispersion $E(\boldsymbol{k})$ and consequently little dispersion $E(\theta)$, since θ is related to the parallel component of $\boldsymbol{k}$ via

$$k_{11} = 0 \cdot 511 \sqrt{E_k} \sin\theta. \tag{1}$$

In equation (1) E_k is the kinetic energy of emission in eV and k_{11} is expressed in Å^{-1}. In contrast, a strongly dispersing band of conduction electrons with s-p symmetry may be identified approaching the Fermi level ($E = 0$) around $\theta = -40°$. This corresponds to the Brillouin zone boundary at $\bar{\mathrm{M}}$(L); the reflection symmetry of this band about the zone boundary (Bragg plane) is also evident. For most angles of emission, however, there is little evidence of emission from the Fermi edge itself—what intensity there is can be readily explained by involving quasi-elastic (phonon) scattering. The obvious exception to this lack of Fermi edge emission is evident in the small symmetric peak located at $\theta = 0$. This is emission from a well documented (Kevan 1983) surface state at Γ. The detailed dispersion of this state is shown in Fig. 2 which provides a good illustration of the energy and angular resolution of the toroidal analyser.

By way of contrast, Fig. 3 illustrates the type of data set which is obtained from typical semiconductors. GaAs(001)[1$\bar{1}$0] is shown in Fig. 3*a* in which

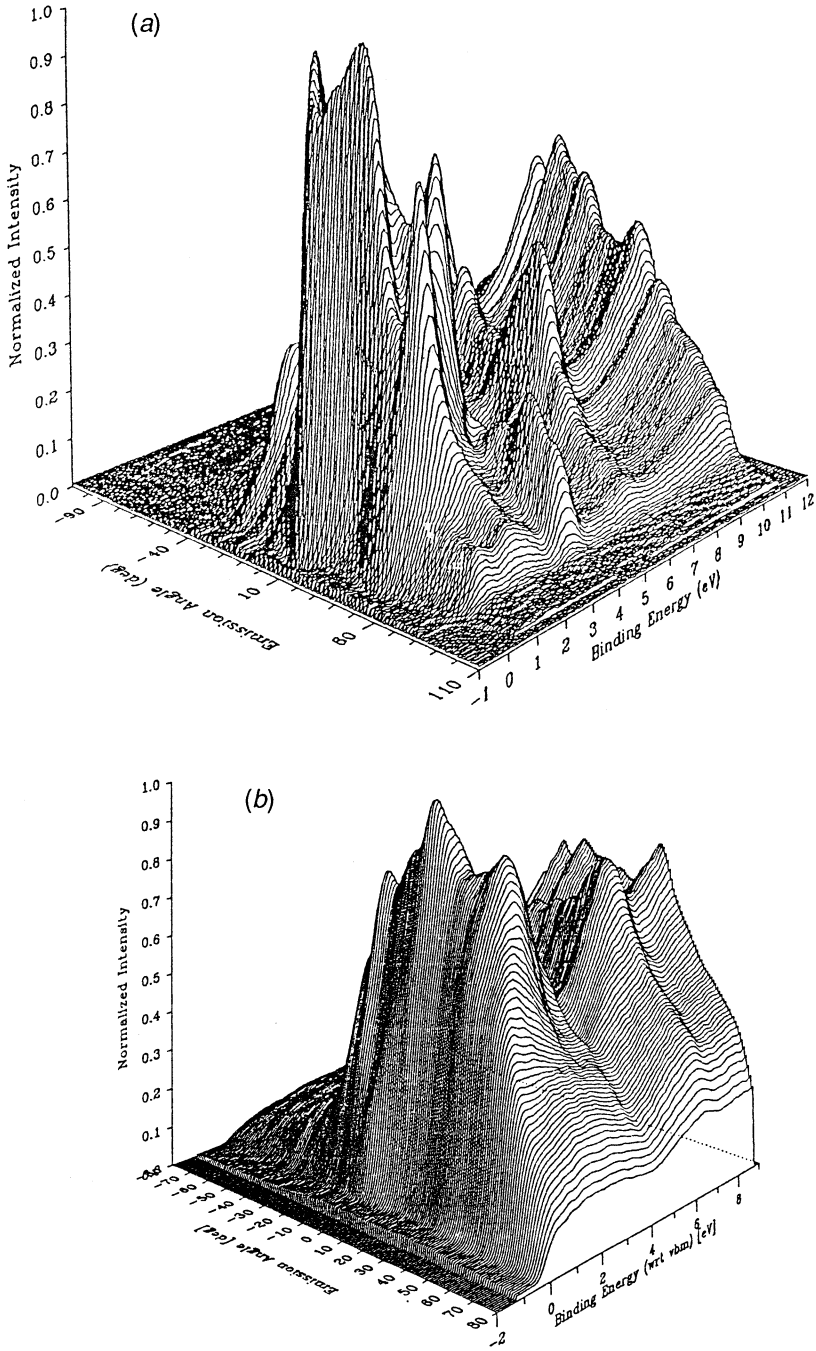

Fig. 3. (*a*) Angle resolved photoemission data set from GaAs(001) in the [1$\bar{1}$0] azimuth. (*b*) Similar data from an MBE-grown sample of the alloy $In_{0.27}Ga_{0.73}As$ (001).

the dispersion of what appears to be the uppermost valence band appears to be evident. We will see below that such a simple explanation is quite inadequate; the data in fact consist of a complex mixture of surface and bulk emission. What is evident from a casual comparison between Figs 3*a* and 3*b* is the increased width of spectral features and the increased contribution from inelastically scattered electrons in (*b*) compared with (*a*). This is also as expected since $In_{0\cdot27}Ga_{0\cdot73}As$ is a random substitutional alloy, i.e. it is a disordered alloy in the sense that the (ordered) metal atom sites are randomly Ga or In filled.

Figs 2 and 3 are examples of data sets taken at a single photon energy. On the basis of equation (1), which expresses the fact that translational symmetry is preserved parallel to the surface of the material, we can clearly derive an $E(K_{11})$ map (although the experiment provides no direct indication of the $k_\perp$ component associated with each transition). This is readily done automatically from the $N(E,\theta)$ data set by detecting the location of each peak $E_i\,\theta_i$ and applying equation (1). This procedure is well suited to the study of quasi-2-dimensional materials such as layer compounds or monolayer adsorbates but is of restricted value when applied to fully 3-dimensional materials where strong dispersion with $k_\perp$ can be expected. Until recently, about the best one could do was to project the 3-dimensional theoretical bandstructure onto the surface plane and judge if the experimental points fell within the predicted regions. Fig. 4 is an example where this procedure works reasonably well: this example therefore shows that the theoretical bandstructure is reasonably correct but does not point the way towards refining that calculation.

To illustrate how we have recently overcome this limitation to the interpretation of fixed photon energy ARUPS, we return to a consideration of GaAs as a prototype semiconductor whose surface and interface properties are of considerable technological importance. An experimental $N(E,\theta)$ plot is shown in contour form in Fig. 5 for the MBE-grown GaAs(001) surface measured in the [110] azimuth at 26 eV photon energy, p-polarisation. Our task is to attempt to predict the major features of this result on the basis of a calculated bandstructure which involves surface as well as bulk states.

The photoexcitation process involves a transition from some occupied state $E_i(\boldsymbol{k}_i)$ to an empty conduction band state $E_f(k_i \pm \boldsymbol{G} \pm \boldsymbol{g})$. Here $\boldsymbol{G}$ is a reciprocal lattice vector of the bulk crystal and $\boldsymbol{g}$ a surface reciprocal lattice vector. Although the excited state bandstructure for GaAs has recently been calculated using a sophisticated layer KKR method, its features 20 eV above E_f resemble free electron final states to a considerable degree. Additionally, the short inelastic mean free path for photoexcited electrons (~5 Å) implies a lifetime for such states in the vicinity of 10^{-15} s. In turn, this implies a lifetime broadening of the photoexcited state typically of the order of $\Delta E = \pm 0\cdot 5$ eV. Thus, for photoelectrons detected with energies greater than ~20 eV, the details of the excited state bandstructure are not detectable and a free electron approximation to these states is an adequate description of the photoelectron process from solids. (Note that this conclusion is not valid in the gas phase, as evidenced by the failure of the Born approximation for the interpretation of electron scattering experiments below a few hundred eV kinetic energy.)

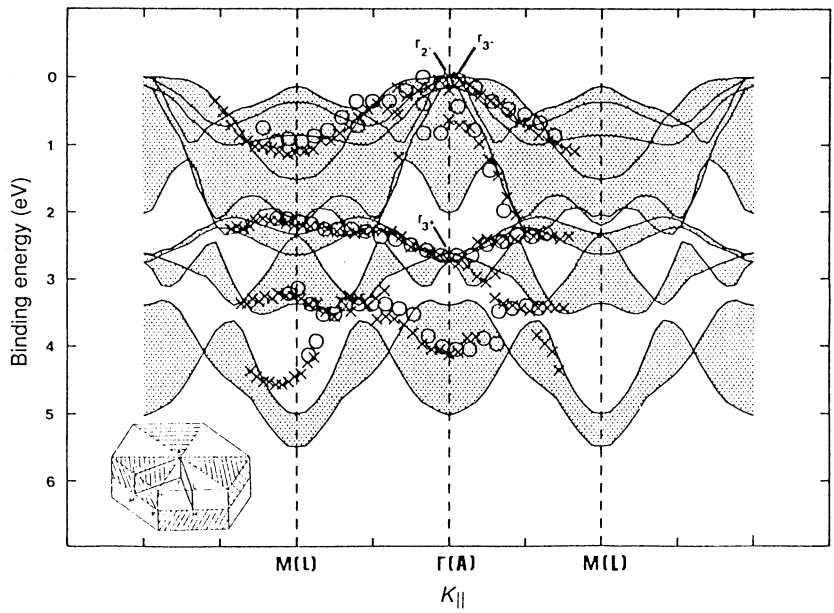

Fig. 4. Experimental energy bands of IT-HfS_2 (crosses HeI, circles NeI) as compared with theoretical bands projected onto the surface plane (from Jakovidis *et al.* 1987).

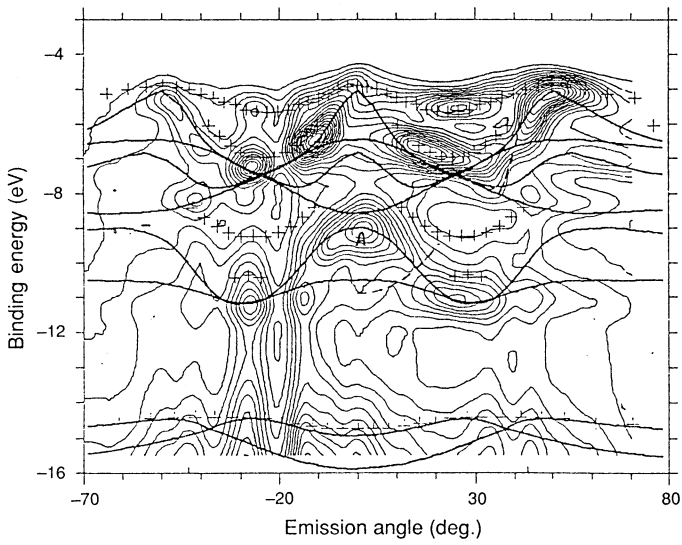

Fig. 5. Contour plot of photoemission from MBE-grown GaAs(001)[110] using p-polarised, 26 eV photons. Solid lines are the predicted loci of observable transitions from bulk eigenstates; crosses are the predicted loci of emission from surface states.

The loci of transitions between the theoretical valence band surface $E_i(k_{11}, k_\perp)$ and appropriate branches of the free electron conduction bands,

$$E_f = \frac{\hbar^2}{2m}(\boldsymbol{k} \pm \boldsymbol{G} \pm \boldsymbol{g})^2 ,$$

may now be determined for the chosen photon energy, thereby identifying the energies and wavevector of the initial states from which photoemission may occur. Using equation (1), the k_{11} values so selected may be converted to polar angle of emission values (θ) for comparison with experiment. The result of this procedure is also shown in Fig. 5, where a distinction is made between transitions from bulk bands as opposed to those from surface states. In the latter case, we have used the calculation of Chadi (1978), whereas the bulk bands involved were those calculated using a LMTO method by Cardona *et al.* (1988).

It is clear from Fig. 5 that essentially all the main features of the experiment can now be related to identifiable transitions and that the bandstructure of GaAs is known across the Brillouin zone with some precision. It is also clear that the surface states play an important role but that, without a detailed analysis such as that shown here, this role cannot readily be distinguished by inspection alone of off-normal data. It is also clear that the emission in the vicincity of the valence band edge, clearly visible in Fig. 3*a*, is in fact dominated by surface rather than bulk bands.

A more traditional approach to bandmapping uses the additional flexibility, available at synchrotron radiation sources, of variable photon energy. A typical set of data from the alloy $In_{0.27}Ga_{0.73}As$ covering the photon energy range $11 < h\nu < 50$ eV is shown in Fig. 6. Dispersion in binding energy with photon energy is clearly visible. Since this is normal emission data, $\theta = k_{11} = 0$ and the dispersion visible is consequently in the $k_\perp$ direction. To establish the actual value of $k_\perp$ associated with each peak in Fig. 6 we use the so-called structure plot approach shown in Fig. 7. We have recently given details of the manner in which the initial state bandstructure $E_i(k)$ is deduced using such a plot (Stampfl *et al.* 1989), but the approach may be summarised as follows. We again assume the adequacy of free-electron final states for kinetic energies greater that ~ 20 eV and use an appropriate (calculated) valence bandstructure in conjunction with these final states to determine an appropriate inner potential and to identify the reciprocal lattice vectors participating in each transition. Ths involves the construction of a theoretical structure plot—as also shown in Fig. 7—which then enables us to produce a corrected valence bandstructure. After some iterations of this procedure we obtain an experimentally derived valence bandstructure and also some indication of the degree to which the free electron approximation fails for energies below 20 eV (see Fig. 8).

To illustrate the current degree of sophistication in such experiments we now consider the effect of lattice strain on the valence bandstructure of InGaAs. This experiment is made possible by the fact that thin (<100 Å) films of $In_{0.27}Ga_{0.73}As$, grown epitaxially on a GaAs(001) substrate, accommodate the 7% mismatch in unit cell size by means of a compression in the plane of the surface with a consequent elongation normal to the surface. The unit

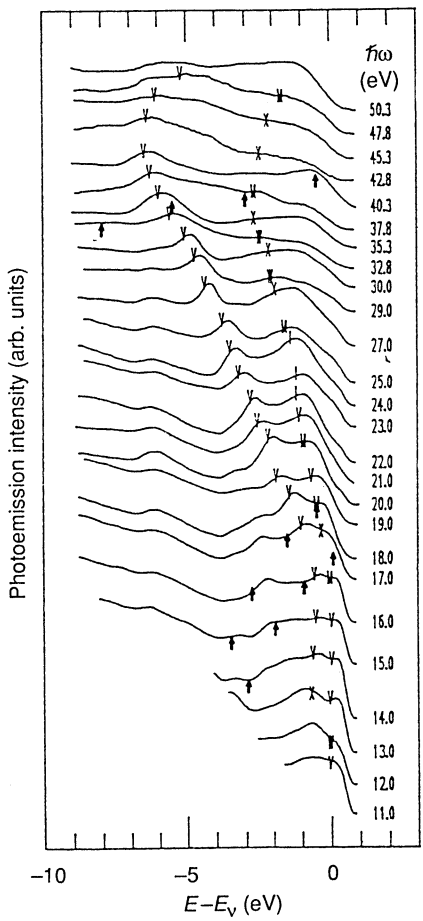

Fig. 6. Normal emission energy distribution curves from $In_{0.27}Ga_{0.73}As(001)$ covering the photon energy 11 to 50 eV. Peaks identified by letters represent emission from the uppermost (bulk) valence bands. Arrows show where artifacts due to second order light may appear.

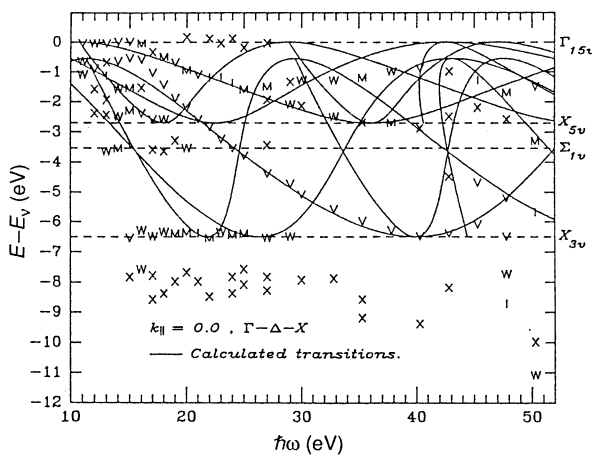

Fig. 7. Structure plot derived from the data of Fig. 6 (crosses) together with the predictions of a model which invokes free-electron-like final state bands. Such a plot enables us to identify the G associated with individual transitions and to specify the inner potential.

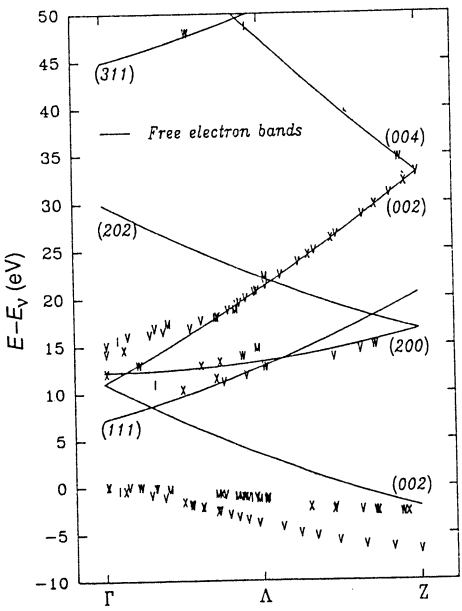

Fig. 8. Experimental valence and conduction bands for $In_{0.27}Ga_{0.73}As(001)$, together with appropriate branches of the free-electron parabola, showing deviations from this model for photon energies less than 20 eV.

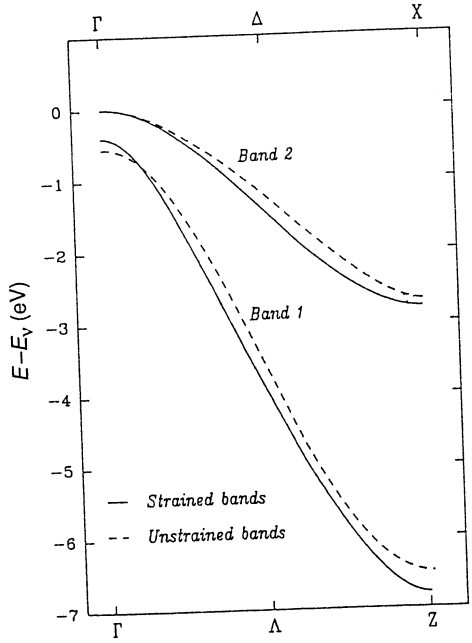

Fig. 9. Valence bands illustrating the effect of strain in $In_{0.27}Ga_{0.73}As$ as derived from a photoemission study (from Stampfl *et al.* 1990).

cell of such strained $In_{0.27}Ga_{0.73}As$ is thus tetragonal. Growth of thicker films on the other hand, results in the production of FCC $In_{0.27}Ga_{0.73}As$ since in this case, the material cannot accommodate the accumulated strain which is consequently relieved by dislocations. We may investigate the effects of this lattice strain on the bandstructure of this material since strained and unstrained samples of otherwise identical material may be grown using the MBE technique. The result of a synchrotron radiation study of InGaAs films analysed by the method briefly outlined above is shown in Fig. 9. The ***k***-dependent differences in the two valence bands are clearly evident in this data. Although calculations for this material are not presently available, strain-induced effects of similar magnitude have recently been predicted for GaAs by Zollner *et al.* (1990).

We now turn to the elucidation of (empty) conduction band states by photoemission and to a consideration of the role of surface and bulk Umklapp scattering mechanisms. We will examine those questions with the help of the newly developed technique of angle resolved constant initial state spectroscopy (ARCIS).

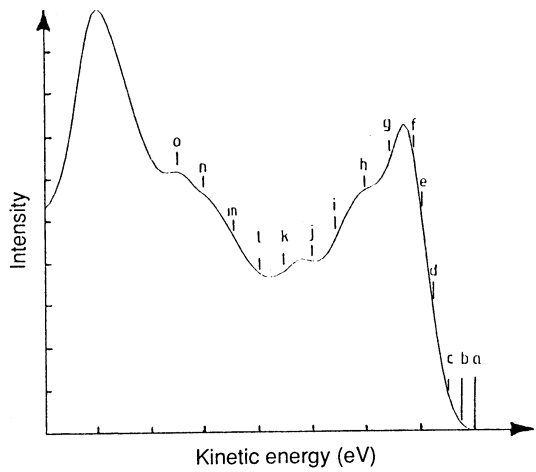

Fig. 10. Normal emission distribution curve from cleaved GaAs(110) at a photon energy of 21 eV (p-polarisation). Labelled points indicate the binding energies at which ARCIS data have been collected.

ARCIS is a technique whereby attention is focussed on emission from a particular initial state energy E_i. The kinetic energy of detection is altered in synchronism with alteration of the photon energy. The resulting spectra therefore reflect the probability of emission from the selected valence state to all available final states. We can consequently learn much about the excited state bandstructure even if only normal emission is investigated: much more information is available if ARCIS data are acquired covering all off-normal angles of emission as well.

In the case of GaAs(110), data were obtained for a large number of initial state energies as indicated in Fig. 10. This shows a normal emission energy

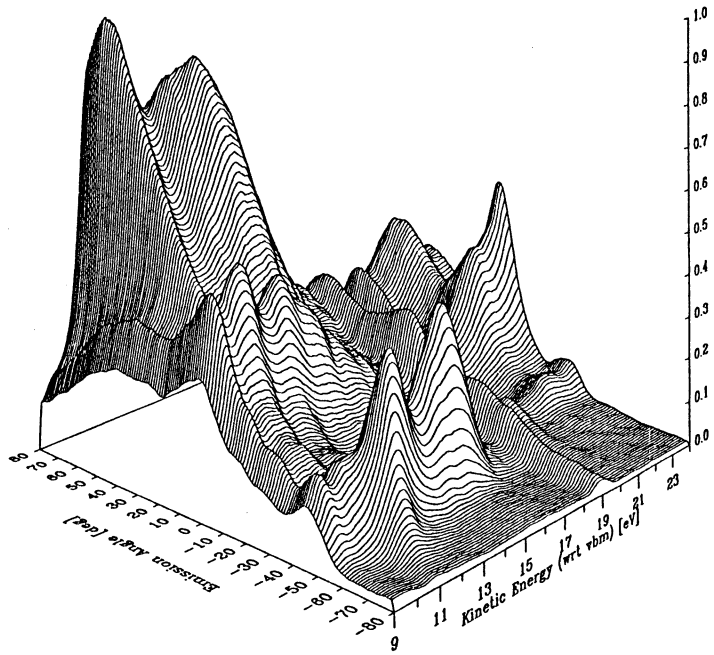

Fig. 11*a*. ARCIS data from the valence band edge of GaAs(110) shown in hidden line form.

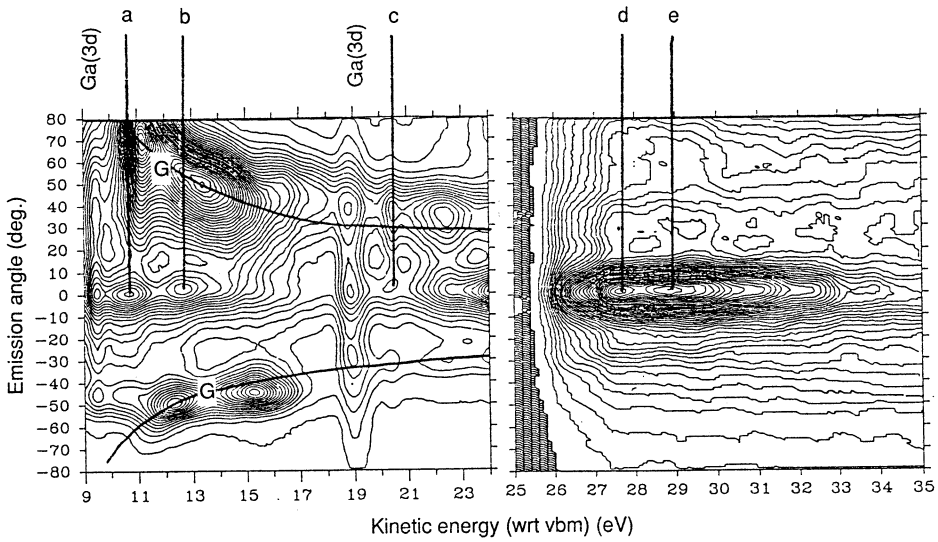

Fig. 11*b*. ARCIS data from the valence band edge of GaAs(110) shown in contour form. The solid lines show $k_{\|} = 1 \cdot 11$ Å^{-1}. The peaks labelled a to e relate to transitions similarly labelled in Fig. 12.

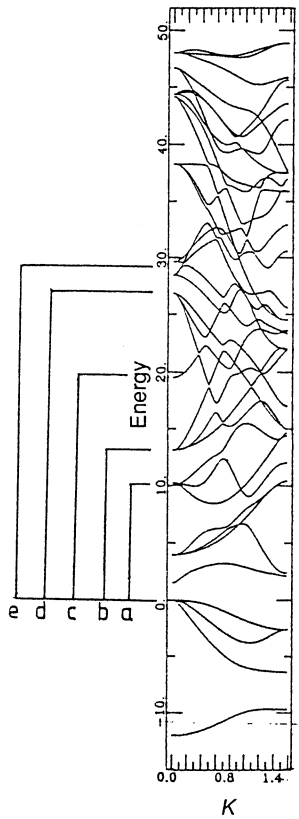

Fig. 12. LMTO bands for the ΓX direction in GaAs (from Cardona *et al.* 1988). Transitions visible in the CIS data of Fig. 11 at normal emission are labelled.

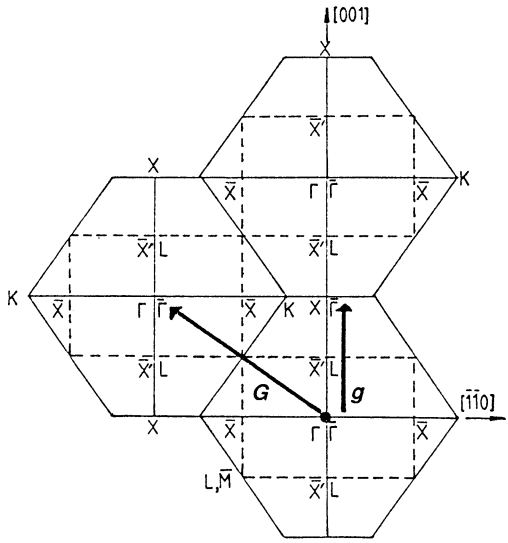

Fig. 13. Surface and bulk reciprocal lattices appropriate to the GaAs(110) surface. It may be seen that the surface zone boundary at $\bar{X}$ is half-way to the bulk zone boundary at X. Surface ***g*** and bulk ***G*** vectors referred to in the text are also shown.

distribution curve taken with a photon energy of 21·0 eV and may be taken as representative of such spectra over a reasonable range of photon energies. Point a is clearly above the valence band maximum and the ARCIS data are dominated by effects due to second order light from the monochromator and are not shown here. For emission from the extreme top of the valence band (point b) we obtain the ARCIS data sets shown in hidden line and in contour form in Fig. 11. Two separate gratings were used to acquire the data of Fig. 11; no attempt has been made to normalise these data or to allow for variations in monochromator efficiency. At normal emission, the peaks labelled a to e in the contour plots correspond well with transitions from Γ to the final state bands as predicted by Cardona *et al.* (1988) (see Fig. 12).

As a example of the additional information which may be extracted from such ARCIS data, the structures labelled G in Fig. 11 can be mentioned. Using equation (1) it is readily shown that these peaks lie on lines of constant $k_{||} = 1 \cdot 11$ Å^{-1}. Referring to Fig. 13, we show the surface Brillouin zone together with the slice through the bulk zone appropriate to a (110) surface. In the measured azimuthal direction, the surface zone dimension is one-half the bulk zone dimension, i.e. $\Gamma X = 0 \cdot 5\, \Gamma X = 1 \cdot 11$ Å^{-1}. The peaks labelled G are therefore associated with scattering involving a momentum transfer of $1 \cdot 11$ Å^{-1} which could occur due to either a surface or a bulk process. Thus, peaks G could be due to surface Umklapp scattering (transfer of $\hbar \boldsymbol{g}$) or they could be indicative of scattering involving a nearest neighbour Γ point of the bulk reciprocal lattice (transfer of $\hbar \boldsymbol{G}$). Although we cannot with certainty distinguish between these possibilities at present, the indications favour a surface mechanism since, as appears to to be the case, the final states associated with these transitions are associated with the bandstructure at X rather than at Γ. ARCIS data from the other initial states labelled in Fig. 10 have also been successfully interpreted in terms of the LMTO bandstructure and will be presented in a forthcoming paper.

3. Summary

The ability of the technique of angle resolved photoemission to investigate the surface and bulk bandstructure of materials has been indicated using primarily semiconductor examples. It has been demonstrated that the accuracy of a theoretical bandstructure may be tested by an ARUPS experiment performed at a single photon energy in a standard laboratory. It has further been demonstrated that, if variable photon energies are available, an experimentally derived bandstructure may be obtained even in cases such as InGaAs where no theoretical calculation exists. The precision of such determinations has been shown to be sufficient to permit the measurement of small, k-dependent, shifts in the valence band produced by the deliberate introduction of lattice strain. ARCIS experiments have been shown to be a valuable check on the validity of the latest excited state bandstructure calculations. Such data also show, in graphic detail, the role played by Umklapp scattering in the photoemission process.

Photoemission from adsorbates is an active and expanding technique which has not been addressed here. Rather, the present paper has attempted to show that photoemission has a vital role to play in understanding the surface

electronic properties of clean surfaces. Nor has attention been paid here to the wealth of information which may be obtained by examining the line shape of core energy levels using somewhat higher photon energies. A review of surface core level shifts of this nature may be found in Egelhoff (1987).

Acknowledgments

The work reviewed here has been the result of the efforts of many people both at LaTrobe University (A. Stampfl, G. Kemister, Y. Q. Cai) and in Germany (L. Ley, J. Fraxedas, F. U. Hillebrecht). The contribution of each has been invaluable. We are also indebted to Prof. Cardona, MPI-F Stuggart, for granting access to the Berlin SR source and to the staff there for much advice and support. Financial support from the ARC (Australia) and BMFT (Germany) is also acknowledged.

References

Cardona, M., Christensen, N., and Fasol, G. (1988). *Phys. Rev.* B **38**, 1806.
Chadi, D. J. (1978). *Phys. Rev.* B **18**, 1800.
Egelhoff, W. F. (1987). *Surf. Sci. Rep.* **6**, 1.
Kevan, S. D. (1983). *Phys. Rev. Lett.* **50**, 526.
Jakovidis, G., Riley, J. D., Liesegang, J., and Leckey, R. C. G. (1987). *J. Elect. Spectrosc. Relat. Phenom.* **42**, 275.
Leckey, R. C. G., and Riley, J. D. (1985). *Appl. Surf. Sci.* **22/23**, 196.
Stampfl, A., Kemister, G., Leckey, R. C. G., Riley, J. D., Order, P. T., Hillebrecht, F. U., Fraxedas, J., and Ley, L. (1989). *J. Vac. Sci. Technol.* A **7**, 2525.
Stampfl, A., Kemister, G., Leckey, R. C. G., Riley, J. D., Orders, P. J., Usher, B., Hillebrecht, F. U., and Ley, L. (1990). *Phys. Scripta* (in press).
Toffoletto, F., Leckey, R. C. G., and Riley, J. D. (1985). *Nucl. Instrum. Methods* B **12**, 282.
Zollner, S., Schmid, U., Grein, C., Christensen, N. E., Cardona, M., and Ley, L. (1990). To be published.

Manuscript received 6 February, accepted 9 May 1990